

Article

# Design for Random Response of Structures Subject to Rhythmic Crowd Loading

Jing-Kun Dong and Mao Ye \*

Wind Engineering and Engineering Vibration Research Center, Guangzhou University, Guangzhou 510006, China

\* Correspondence: yemao@gzhu.edu.cn

**Abstract:** Overall, this paper provides a comprehensive approach for designing structures subject to rhythmic crowd loading. By considering the randomness of the load model and structural response, the design method provides a more realistic evaluation of the structure's performance. The establishment of links between the deterministic individual loading and the random crowd loading simplifies the calculation process and makes it more practical for real-world applications. The use of reduction factors based on experimentally determined standard deviations ensures that the design method provides a lower bound for the expected response of the structure. The consideration of the involvement of an infinite number of people in the reduction factors adds an additional level of conservatism to the design, further ensuring the safety of the structure. The examples provided illustrate the effectiveness of the design method in evaluating the maximum displacements and accelerations of a floor structure subjected to rhythmic crowd loading. Overall, the paper provides a valuable contribution to the field of structural engineering by providing a practical and realistic approach for designing structures subject to rhythmic crowd loading.

**Keywords:** rhythmic crowd loading; designing structures; expected response



**Citation:** Dong, J.-K.; Ye, M. Design for Random Response of Structures Subject to Rhythmic Crowd Loading. *Buildings* **2023**, *13*, 1085. <https://doi.org/10.3390/buildings13041085>

Academic Editor: Francisco López-Almansa

Received: 29 March 2023

Revised: 14 April 2023

Accepted: 16 April 2023

Published: 20 April 2023



**Copyright:** © 2023 by the authors. Licensee MDPI, Basel, Switzerland. This article is an open access article distributed under the terms and conditions of the Creative Commons Attribution (CC BY) license (<https://creativecommons.org/licenses/by/4.0/>).

## 1. Introduction

Rhythmic crowd loading refers to the repeated and organized movements of a group of people, such as in a dance or exercise class. This type of loading can cause resonant vibrations in lightweight structures, which can be dangerous if not properly accounted for in the design phase. The study of dynamic behaviour induced by crowd loading has become increasingly important in recent years due to the growing popularity of large public spaces, such as stadiums and concert halls. These spaces are often designed to accommodate large numbers of people, and therefore must be able to withstand the dynamic loads induced by crowd movement. In addition to safety concerns, serviceability is also an important factor in the design of these structures. Vibrations induced by crowd loading can be felt by other users of the space, such as spectators or workers, and can cause discomfort or even nausea. In summary, understanding the dynamic behaviour of lightweight structures induced by crowd loading is crucial for ensuring both the safety and comfort of users in large public spaces. The importance of this has been highlighted by SCOSS [1]. Further research in this area will continue to be important as these spaces become more common and more heavily used.

This type of loading can be observed in various settings, such as concerts, sports events, festivals, and dance parties. The rhythmic crowd loading can cause significant dynamic forces on the structure. Organizers should ensure that the structure and equipment are designed to withstand the expected loads. The crowd load is very uncertain; Luca Bruno proposed that the influence of a large number of uncertain parameters should be considered in the probabilistic response research and reliability analysis of pedestrian excitation structures [2]. In addition, engineers can use advanced analytical tools, such as finite element analysis, to simulate crowd behaviour and predict the induced forces.

Some individual rhythmic loads on a structure have been intensively studied, such as individual jumping loads [3–6] and individual bouncing loads [6–9]. Crowd jumping loads have also been studied [10,11]. The rhythmic crowd load can be quite a serious load case, especially as it may generate a resonant reaction in some structures. Angitha Vijayan suggested that if there is a mode with low natural frequency, even a very low forced frequency will lead to strong vibration, which may lead to panic [12]. Bruno and Venuti proposed a model to describe the behavior of unrelated and synchronous pedestrians by linking the percentage of synchronous pedestrians with the crowd density value [13]. Structural responses induced by rhythmic loading have also been investigated. Ji and Ellis [14] provided an analytical method for determining the response of floors to these loads. The analytical method was verified by the experiment in [15]. Willford [16] carried out an investigation into crowd-induced vertical dynamic loads using available measurements. Gaspar and Silva [17] studied the structural problems related with excessive vibrations of steel–concrete composite floors due to human rhythmic activities. However, as rhythmic loads are applied on the structures, taking into consideration the proposed recommendations by Annex A in BS 6399 Part 1 [18], it always results in a much higher structural response than that found in practice [19] to data. One reason for overestimation is the significant difference between the situation where everyone is doing the coordinated actions and the situation where only some of the crowd are doing the coordinated actions, which is often encountered in a practical situation. For example, in pop concerts, some people are jumping and other people are just bouncing or bobbing. These two cases result in large differences in the structural vibration. In this paper, the extreme case when everyone in a crowd is doing the coordinated actions is considered. Another reason is that perfect synchronism is unlikely even when there is a music beat to follow when a crowd of people attempt the same repetitive movement. The imperfection in coordination is mainly due to that in responding to music beats, individuals may move slightly faster or slower, or move higher or lower. Imperfect synchronism is intensively considered in the analysis of the random response of structures subject to rhythmic crowd loading in this paper.

The paper investigates the design method for evaluating random responses of structures subject to rhythmic crowd loading. The proposed design method can be applied to a range of structures, such as grandstands, bridges, and floors subject to crowd loading, when the response of a structure is dominated by its single (normally fundamental) mode. The method provides valuable insights into the effects of imperfect synchronism and the potential reduction in resonant response due to the damping effect of crowd loading. The analysis highlights the importance of accounting for the randomness of crowd behavior and its impact on structural response, which is critical for the safety and reliability of the structures. Overall, the proposed design method can aid in the development of safer structures in crowded settings, making them more resilient to the effects of crowd loading.

## 2. Random Load Model

An individual dance-type load where jumping is included can be described as follows

$$F(t) = G \left[ 1.0 + \sum_{n=1}^{\infty} r_n(\alpha) \sin(2\pi f_p t + \phi_n) \right] \quad (1)$$

where  $f_p = 1/T_p$  is the load frequency and  $G$  is the individual body weight.  $r_n$  and  $\phi_n$  are the Fourier coefficient and the phase lag, respectively, defined by Ji and Ellis [14]. Both  $r_n$  and  $\phi_n$  are functions of the contact ratio  $\alpha$  corresponding to different activities.  $r_n$  is defined below

$$r_n(\alpha) = \begin{cases} \pi/2 & \text{for } 2n\alpha = 1 \\ \left| \frac{\cos(n\pi\alpha)}{1-4n^2\alpha^2} \right| & \text{for } 2n\alpha \neq 1 \end{cases} \quad (2)$$

$$\phi_n(\alpha) = \begin{cases} 0 & \text{for } n\alpha = 1/2 \\ \tan^{-1}\left(\frac{1+\cos(2n\pi\alpha)}{\sin(2n\pi\alpha)}\right) + \pi & \text{for } \frac{\sin(2n\pi\alpha)}{1-(2n\alpha)^2} < 0 \\ \tan^{-1}\left(\frac{1+\cos(2n\pi\alpha)}{\sin(2n\pi\alpha)}\right) & \text{for } \frac{\sin(2n\pi\alpha)}{1-(2n\alpha)^2} > 0 \end{cases} \quad (3)$$

The load model for an individual jumping has been experimentally verified [15]. When  $M$  people in a group move, perfect coordination between individuals in the group is unlikely to be achieved. As a result, the load model for an individual jumping may not be directly applicable to a group of people moving together. The imperfection in coordination is mainly due to that in responding to music beats, individuals may move slightly faster or slower by  $\Delta t_s$  or jump higher or lower by  $\Delta a$ .  $\Delta f_p$  describes the random difference between the music beat frequency and the frequency that a person jumps;  $\Delta t_s$  indicates that even if people move at the music frequency, they may move randomly a little ahead or behind the music beat; and  $\Delta a$  shows that people may jump higher or lower than the average contact ratio in the group. Therefore, it is assumed that  $\Delta f_p$ ,  $\Delta t_s$ , and  $\Delta a$  are the three independent random variables.  $\Delta a$ ,  $\Delta t_s$ ,  $\Delta f_p$  attenuate the structural response. Following this assumption, the load induced by the typical  $s$ th individual in the group becomes

$$F_s(t) = G_s \left[ 1.0 + \sum_{n=1}^{\infty} r_n(\alpha + \Delta\alpha) \sin(2n\pi(f_p + \Delta f_p)t + \phi_n + n\psi) \right] \quad (4)$$

where  $\psi = 2\pi\Delta t_s/T_p$  is a phase lag variation, which characterizes the phase difference between an individual in a group and the music beat played.

When  $M$  people in a group move, the load becomes

$$F(t) = \sum_{s=1}^M G_s \left[ 1.0 + \sum_{n=1}^{\infty} r_n(\alpha + \Delta\alpha) \sin(2n\pi f_p t + \phi_n + n\psi) \right] \delta(x - x_s) \delta(y - y_s) \quad (5)$$

where  $\delta(\bullet)$  is a Dirac function.

As people in the group tend to follow the music as accurately as possible, the time delay variation  $\psi$  is expected to follow the normal distribution

$$f(\psi) = \frac{1}{\sigma_\psi \sqrt{2\pi}} e^{-(\psi - \mu_\psi)^2 / 2\sigma_\psi^2} \quad (6)$$

where  $\mu_\psi$  is the mean of time delay variation  $\psi$  and is zero ( $\mu_\psi = 0$ ); the parameter  $\sigma_\psi$  is its standard deviation, and

$$\psi \in [-\pi, \pi] \quad (7)$$

### 3. Random Responses of a Structure

When the response of a structure, such as floors and grandstands, is dominated by its single (normally fundamental) mode subject to dance-type loads (Equation (1)), a method for calculating the responses of the generalised single degree of freedom system has been provided [14]. The displacement of the generalised SDOF system induced by an individual (Equation (1)) is

$$A_s(t) = \frac{G_s W(x_s, y_s)}{K^*} \left[ 1.0 + \sum_{n=1}^{\infty} \frac{r_n(\alpha) \sin(2n\pi f_p t + \phi_n - \theta_n)}{\sqrt{(1 - (n\beta)^2)^2 + (2n\zeta\beta)^2}} \right] \quad (8)$$

where  $W(x, y)$  is the mode shape of the structure,  $G_s W(x_s, y_s)$  is the modal load, and  $K^*$  is the modal stiffness of the generalised SDOF system.  $\beta$  is the ratio of the load frequency to the frequency of the generalised SDOF system, i.e.,  $\beta = f_p/f_s$ .  $f_s$  is the frequency of the generalised SDOF system.  $\theta_n$  is the phase angle,  $\theta_n = \tan^{-1}(2\zeta n\beta / (1 - (n\beta)^2))$ .

The ratio after the summation sign is the conventional response of the SDOF system subject to a harmonic load, and the summation considers the effect of several harmonic load components in Equation (1).

When a group of people jumps in perfect coordination, the displacement and acceleration response induced by the group just simply sums up the response induced by an individual (Equation (8)) as follows:

$$A_I(t) = \frac{\sum_{s=1}^M G_s W(x_s, y_s)}{K^*} \left[ 1.0 + \sum_{n=1}^{\infty} \frac{r_n(\alpha) \sin(2n\pi f_p t + \phi_n - \theta_n)}{\sqrt{(1 - (n\beta)^2)^2 + (2n\zeta\beta)^2}} \right] \quad (9)$$

$$\ddot{A}_I(t) = \frac{\sum_{s=1}^M G_s W(x_s, y_s)}{K^*} \sum_{n=1}^{\infty} \frac{(2n\pi f_p)^2 r_n(\alpha) \sin(2n\pi f_p t + \phi_n - \theta_n)}{\sqrt{(1 - (n\beta)^2)^2 + (2n\zeta\beta)^2}} \quad (10)$$

When the same generalised SDOF system is considered subject to the random individual load (Equation (5)) with  $\Delta\alpha$ ,  $\Delta t$ , and  $\Delta f_p$ , the random displacement of the generalised SDOF system becomes similar to Equations (8) and (9),

$$A_R(t) = \frac{\sum_{s=1}^M G_s W(x_s, y_s)}{K^*} \left[ 1.0 + \sum_{n=1}^{\infty} \frac{r_n(\alpha + \Delta\alpha) \sin(2n\pi f_p t + \phi_n + n\psi - \theta_n)}{\sqrt{(1 - (n\beta(1 + \lambda))^2)^2 + (2\zeta n\beta(1 + \lambda))^2}} \right] \quad (11)$$

where  $\lambda$  is the ratio of the frequency variation  $\Delta f_p$  to the load (or music) frequency  $f_p$ , i.e.,  $\lambda = \Delta f_p / f_p$ .

At the resonant situation,  $n f_p = f_s$ , then

$$n\beta = 1 \quad (12)$$

As people in the group tend to jump to the music beat as accurately as possible, the frequency variation  $\lambda$  is expected to follow a normal distribution

$$f(\lambda) = \frac{1}{\sigma_\lambda \sqrt{2\pi}} e^{-(\lambda - \mu_\lambda)^2 / 2\sigma_\lambda^2} \quad (13)$$

where  $\lambda$  is defined in Equation (11).  $\mu_\lambda$  is the mean of frequency variation and is zero ( $\mu_\lambda = 0$ ); the parameter  $\sigma_\lambda$  is its standard deviation, and

$$\lambda \in [-0.5, 0.5] \quad (14)$$

As with the time delay variation and the frequency variation, the contact ratio variation  $\delta$  is also expected to follow a normal distribution

$$f(\delta) = \frac{1}{\sigma_\delta \sqrt{2\pi}} e^{-(\delta - \mu_\delta)^2 / 2\sigma_\delta^2} \quad (15)$$

where  $\delta = \Delta\alpha$ ,  $\mu_\delta$  is the mean of frequency variation  $\Delta\alpha$  and is zero ( $\mu_\delta = 0$ ); the parameter  $\sigma_\delta$  is its standard deviation, and

$$\delta \in [-0.5, 0.5] \quad (16)$$

#### 4. Evaluation of Random Responses

It is difficult to calculate the random responses  $A_R(t)$  in design. Therefore, the provision of the mean responses  $E[A_R(t)]$  of the structure is expected. It is assumed that  $\Delta f_p$ ,  $\Delta t_s$ , and  $\Delta a$  are the three independent random variables at the beginning of this paper.

Meanwhile, the randomness for the phase lag  $\phi_n$  and phase angle  $\theta_n$  is not considered in the evaluation of the structural random response. Therefore, the mean of the random displacement  $A_R(t)$  of the structure shown in Equation (11) is

$$E[A_R(t)] = \frac{\sum_{s=1}^M G_s W(x_s, y_s)}{K^*} \left[ 1.0 + \sum_{n=1}^{\infty} C_\delta(n) C_\psi(n) C_\lambda(n, \xi) \frac{r_n(\alpha) \sin(2n\pi f_p t + x\phi_n - \theta_n)}{\sqrt{(1 - (n\beta(1 + \lambda))^2)^2 + (2\xi n\beta(1 + \lambda))^2}} \sin(2n\pi f_p t + \phi_n - \theta_n) \right] \quad (17)$$

where  $C_\delta(n)$  reflects the significance of the contact ratio effect, it is named as the synchronization reduction factor;  $C_\psi(n)$  describes the significance of the dynamic crowd effect, named as the crowd reduction factor;  $C_\lambda(n, \xi)$  can be seen as the frequency reduction factor and is a function of the critical damping ratio of the generalised SDOF system. Three reduction factors are defined by

$$C_\psi(n) = \frac{1}{\sigma_\psi \sqrt{2\pi}} \int_{-\pi}^{\pi} \cos(n\psi) e^{\frac{-\psi^2}{2\sigma_\psi^2}} d\psi \quad (18)$$

$$C_\delta(n) = \frac{1}{\sigma_\delta \sqrt{2\pi}} \int_{-0.5}^{0.5} \left| \frac{\cos(n\pi(\alpha + \delta))}{1 - (2n(\alpha + \delta))^2} \right| e^{\frac{-\lambda^2}{2\sigma_\delta^2}} d\delta \quad (19)$$

$$C_\lambda(n, \xi) = \frac{1}{\sigma_\lambda \sqrt{2\pi}} \int_{-0.5}^{0.5} \frac{\sqrt{(1 - (nf_p/f)^2)^2 + (2\xi(nf_p/f))^2}}{\sqrt{(1 - (nf_p/f)^2(1 + \lambda))^2 + (2\xi(nf_p/f)(1 + \lambda))^2}} e^{\frac{-\lambda^2}{2\sigma_\lambda^2}} d\lambda \quad (20)$$

When deriving Equation (18), the following equation about the time delay variation  $\psi$  is used

$$\int_{-\pi}^{\pi} \sin(n\psi) e^{\frac{-\psi^2}{2\sigma_\psi^2}} d\psi = 0 \quad (21)$$

Equation (17) indicates that the calculation of the mean value of the response is equivalent to that of the mean values of the magnification factor independently.

The mean acceleration can be obtained by differentiating twice  $E[A_R(t)]$  in respect to time and is given as follows:

$$E[\ddot{A}_R(t)] = \frac{\sum_{s=1}^M G_s W(x_s, y_s)}{K^*} \sum_{n=1}^{\infty} (2n\pi f_p)^2 C_\delta(n) C_\psi(n) C_\lambda(n, \xi) \sin(2n\pi f_p t + \phi_n - \theta_n) \quad (22)$$

## 5. Evaluation of Reduction Factor

In some practical experiences, it is found that the first two or three loading components are significant when a crowd is considered. This indicates that only the first three Fourier terms need to be considered in the analysis and design. Therefore, the first four Fourier terms are to be considered in the flowing analysis. Meanwhile, it is found that some experimental results are used in the evaluation of the reduction factor, and these points include some of the background about the experimental results:

- The frequency around 2 Hz is the easiest frequency for people jumping with rhythm. Therefore, all experimental results in this paper are based on the person's jumping at near 2 Hz.
- Actually, a person jumping by himself should be different for a person jumping in a group. It is considered the same in this paper. This means all experimental results are based on the individual person jumping.

### 5.1. Crowd Reduction Factor

The crowd reduction factor is defined by Equation (18), which considers an infinite number of people involved. In actual situations, the number of jumpers may range from a few tens at aerobics to several thousands in pop concerts. Therefore, the crowd reduction factor evaluated from Equation (18) provides a lower bound, i.e., the actual value of the crowd reduction factor will not be less than the one obtained from Equation (18). The crowd reduction factor depends on the value of the standard deviation  $\sigma_\psi$  and the order of the Fourier terms. For appreciation of the variation of  $C_\psi(n)$  on  $\sigma_\psi$ , several values of the standard deviation are considered.  $\sigma_\psi = 0.22\pi$  for the standard deviation was suggested by Ellis [20] based on the measurements of group jumping tests [21]. The group size ranged from 2 to 64. Another value is given by Jun Chen, etc. in [22]; according to the experiments presented,  $\sigma_\psi$  equals  $0.32\pi$  at 2 Hz. Therefore, some values of standard deviation are selected based on the reference values for evaluating the crowd reduction factor.  $C_\psi(n)$  with respect to  $\sigma_\psi$  is presented in Figure 1. Table 1 lists the first four crowd reduction factors ( $n = 1, 2, 3,$  and  $4$ ) corresponding to five selected values of the standard deviation.

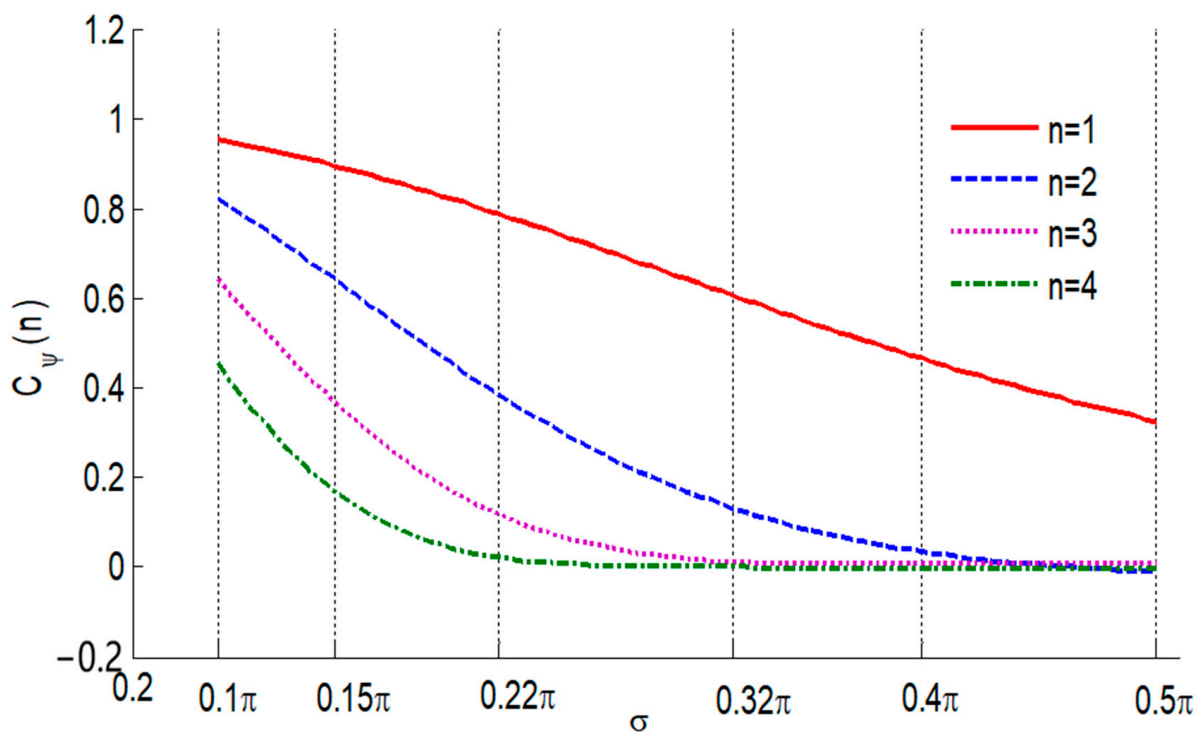


**Figure 1.** Crowd reduction factors  $C_\psi(n)$ .

**Table 1.** Crowd reduction factors  $C_\psi(n)$ .

| $n$ | $\sigma_\psi$ |           |           |           |           |           |           |
|-----|---------------|-----------|-----------|-----------|-----------|-----------|-----------|
|     | $0.20\pi$     | $0.22\pi$ | $0.25\pi$ | $0.28\pi$ | $0.30\pi$ | $0.32\pi$ | $0.35\pi$ |
| 1   | 0.821         | 0.788     | 0.735     | 0.680     | 0.642     | 0.605     | 0.550     |
| 2   | 0.454         | 0.385     | 0.291     | 0.212     | 0.169     | 0.131     | 0.086     |
| 3   | 0.169         | 0.117     | 0.062     | 0.031     | 0.019     | 0.012     | 0.007     |
| 4   | 0.042         | 0.022     | 0.007     | 0.002     | 0.000     | 0.000     | 0.000     |

It can be noted from Figure 1 and Table 1 that:

- The smaller the standard deviation, the larger the crowd reduction factor, which corresponds to better coordination between individuals in a group and a smaller dynamic crowd effect.

- The higher order the load term, the smaller the crowd reduction factor, and the larger the dynamic crowd effect.
- For the range of standard deviation between  $0.22\pi$  and  $0.32\pi$ ,  $C_\psi(3)$  is small and  $C_\psi(4)$  is very small and negligible. This indicates that only the first three Fourier terms need to be considered in the analysis and design. This coincides with practical experience in which only the first two or three loading components are significant when a crowd is considered.

### 5.2. Synchronization Reduction Factor

Similar to the determination of the crowd reduction factor, the evaluation of the synchronization reduction factor considers an infinite number of people. Therefore, the synchronization reduction factor evaluated by Equation (19) provides a lower bound, i.e., the actual reduction factor will not be less than the one evaluated. However, the synchronization reduction factor depends on the standard deviation of the random variable, the average contact ratio  $\alpha$ , and the order of the Fourier terms. A value of the standard deviation of  $\sigma_\delta = 0.082$  Hz was provided when people jumped at [1.9 Hz–2.15 Hz] by Ellis [20]. Another value of the standard deviation of the contact ratio variation  $\delta$  is 0.084 at 2 Hz given by Jun Chen, etc. [22], according to the experiments presented. A value of the average contact ratio  $\alpha = 0.47$  Hz was provided when people jumped at 1.9 by Ellis and Ji [4]. Another value of the contact ratio variation  $\delta$  is 0.67 at 2 Hz given by Jun Chen, etc. [23], according to the experiments. Figure 2 shows the synchronization reduction factor  $C_\delta(n)$  with respect to the standard deviation of the frequency variation  $\sigma_\delta$  and the average contact ratio  $\alpha$  for different orders of the Fourier terms. For a clearer understanding of the effect of  $\sigma_\delta$ , Table 2 lists the first four crowd reduction factors ( $n = 1, 2, 3,$  and  $4$ ) corresponding to five selected values of the standard deviation at  $\alpha = 0.47$ .

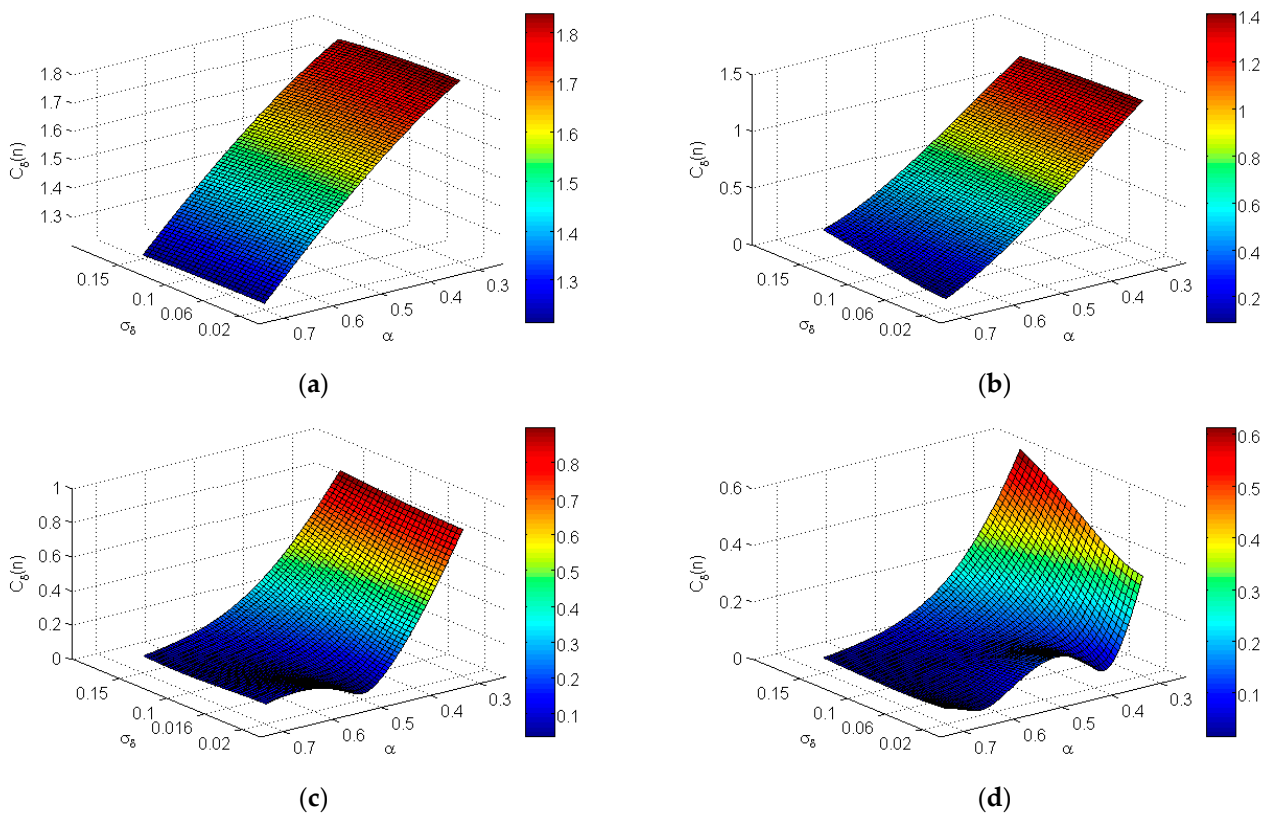


**Figure 2.** Crowd reduction factor  $C_\psi(n)$ . (a)  $n = 1$ . (b)  $n = 2$ . (c)  $n = 3$ . (d)  $n = 4$ .

**Table 2.** Synchronization reduction factors  $C_\delta(n)$ .

| $n$ | $\sigma_\delta$ |       |       |       |       |
|-----|-----------------|-------|-------|-------|-------|
|     | 0.06            | 0.07  | 0.08  | 0.09  | 0.10  |
| 1   | 1.613           | 1.612 | 1.610 | 1.608 | 1.606 |
| 2   | 0.781           | 0.783 | 0.785 | 0.787 | 0.790 |
| 3   | 0.157           | 0.179 | 0.200 | 0.222 | 0.243 |
| 4   | 0.111           | 0.109 | 0.110 | 0.114 | 0.122 |

It can be noted from Figure 2 and Table 2 that:

- Normally, the larger the average contact ratio  $\alpha$ , the smaller the synchronization reduction factor, and the bigger the dynamic crowd effect. However, for  $C_\delta(3)$  and  $C_\delta(4)$  in the area of a lower  $\alpha$  and larger  $\sigma_\delta$ ,  $C_\delta(n)$  is a little bit large.
- The effect of  $\sigma_\delta$  on  $C_\delta(n)$  is not significant, especially for  $C_\delta(1)$  and  $C_\delta(2)$ .
- The larger the order of the Fourier terms, the smaller the synchronization reduction factor, and the bigger the dynamic crowd effect.
- Comparing  $C_\delta(1)$  and  $C_\delta(2)$ ,  $C_\delta(3)$  and  $C_\delta(4)$  is small. This coincides with practical experience in which only the first two or three loading components are significant when a crowd is considered.

Table 3 lists the first four crowd reduction factors ( $n = 1, 2, 3$ , and 4) corresponding to five selected values of the contact ratio  $\alpha$ .

**Table 3.** Synchronization reduction factors  $C_\delta(n)$  with different contact ratios  $\alpha$ .

| $n$ | $\alpha$ |       |       |       |       |
|-----|----------|-------|-------|-------|-------|
|     | 0.3      | 0.4   | 0.5   | 0.6   | 0.7   |
| 1   | 1.827    | 1.708 | 1.564 | 1.400 | 1.222 |
| 2   | 1.387    | 1.036 | 0.680 | 0.367 | 0.151 |
| 3   | 0.863    | 0.406 | 0.152 | 0.111 | 0.096 |
| 4   | 0.455    | 0.161 | 0.099 | 0.060 | 0.043 |

### 5.3. Frequency Reduction Factor

In Equation (20), the frequency reduction factor depends on the value of the standard deviation  $\sigma_\lambda$ , damping ratio  $\zeta$ , the order of Fourier term  $n$ , and the frequency ratio  $f_p/f_s$ . The most critical situation is that resonance occurs, i.e.,  $n f_p/f_s = 1$ , when structures are loaded by rhythmic crowd loading. In this paper, the first four Fourier terms are considered, and the structure is dominated by its single (normally fundamental) mode. Hence, the resonance can occur at the first Fourier term ( $f_p/f_s = 1$ ), the second Fourier term ( $f_p/f_s = 1/2$ ), the third Fourier term ( $f_p/f_s = 1/3$ ), or the fourth Fourier term ( $f_p/f_s = 1/4$ ). It is found that the other three terms  $f_p/f_s$  are ascertained when the resonance term is determined. Table 4 presents the result.

**Table 4.** Based on the resonance term.

| The Resonance Term | $n$ |     |     |     |
|--------------------|-----|-----|-----|-----|
|                    | 1   | 2   | 3   | 4   |
| 1st Fourier term   | 1   | 2   | 3   | 4   |
| 2nd Fourier term   | 1/2 | 1   | 3/2 | 2   |
| 3rd Fourier term   | 1/3 | 2/3 | 1   | 4/3 |
| 4th Fourier term   | 1/4 | 1/2 | 3/4 | 1   |

Now, the resonance term is analysed as follows. Equation (20) becomes

$$C_\lambda(\xi) = \frac{1}{\sigma_\lambda \sqrt{2\pi}} \int_{-0.5}^{0.5} \frac{1}{\sqrt{\left(1 - (1 + \lambda)^2\right)^2 + (2\xi(1 + \lambda))^2}} e^{\frac{-\lambda^2}{2\sigma_\lambda^2}} d\lambda \tag{23}$$

$C_\lambda(\xi)$  is named as the resonance reduction factor. Similar to the crowd reduction factor and the synchronization reduction factor, the resonance reduction factor evaluated by Equation (23) provides a lower bound, i.e., the actual reduction factor will not be less than the one evaluated. However, the resonance reduction factor depends on the standard deviation of the random variable and damping ratio. A value of the standard deviation of  $\Delta f_p = 0.074$  Hz was provided when people jumped at 1.9 Hz by Ellis [22]. This value is equivalent to  $\sigma_\lambda = 0.039$ . Another value of the standard deviation of the frequency variation  $\sigma_\lambda$  is 0.057 at 2 Hz given by Jun Chen, etc. [23], according to the experiments presented. Figure 3 shows the resonance reduction factor  $C_\lambda(\xi)$  with respect to the standard deviation of the frequency variation  $\sigma_\lambda$  and the damping ratio  $\xi$ . For a clearer understanding of the effect of  $\sigma_\lambda$  and  $\xi$ , several values are presented in Table 5.

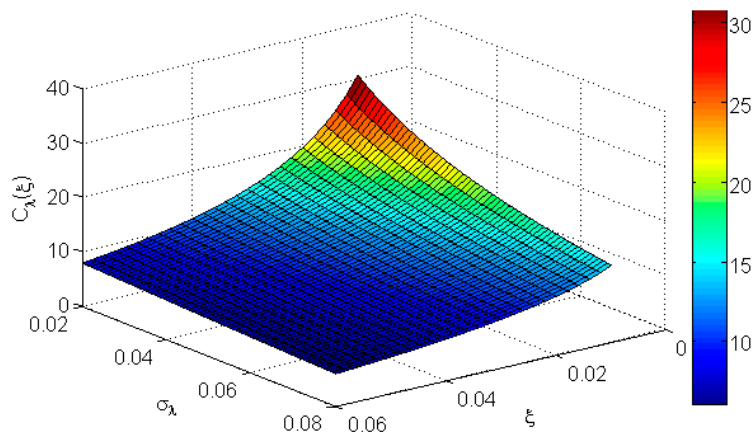


Figure 3. The resonance reduction factor  $C_\lambda(\xi)$ .

Table 5. Several values for the resonance reduction factors  $C_\lambda(\xi)$  ( $n f_p / f_s = 1$ ).

| $\sigma_\lambda$ | $\xi=0.02$ | $\xi=0.03$ | $\xi=0.04$ | $\xi=0.05$ |
|------------------|------------|------------|------------|------------|
| 0.03             | 17.268     | 13.165     | 10.618     | 8.877      |
| 0.04             | 15.358     | 12.017     | 9.876      | 8.373      |
| 0.05             | 13.860     | 11.054     | 9.217      | 7.903      |
| 0.06             | 12.655     | 10.243     | 8.639      | 7.477      |

It can be noted from Figure 3 and Table 5 that:

- The larger the standard deviation, the smaller the resonance reduction factor, and the bigger the dynamic crowd effect.
- The larger the critical damping ratio, the bigger the resonance reduction factor, and the smaller the dynamic crowd effect.

According to Equation (20) and numerical analysis, it is found that the influence of the standard deviation of the frequency variation  $\sigma_\lambda$  and the damping ratio  $\xi$  on the off-resonance reduction factors  $C_\lambda(n, \xi)$  ( $n f_p / f_s \neq 1$ ) is negligible. Several values are presented in Table 6.

**Table 6.** The off-resonance reduction factors  $C_\lambda(n, \xi)$  ( $nf_p/f_s \neq 1$ ).

| $nf_p/f_s$ |       |       |       |       |       |       |       |       |       |
|------------|-------|-------|-------|-------|-------|-------|-------|-------|-------|
| 1/4        | 1/3   | 1/2   | 2/3   | 3/4   | 4/3   | 3/2   | 2     | 3     | 4     |
| 1.067      | 1.125 | 1.334 | 1.806 | 2.310 | 1.339 | 0.828 | 0.337 | 0.126 | 0.068 |

## 6. Example for Evaluation of Random Response of Structure

In this section, the evaluation of the random response of the structure is presented in Tables 1–6. Consider a simply supported floor subject to rhythmic crowd loading, which has the following data:

|                         |                                       |
|-------------------------|---------------------------------------|
| Dimensions:             | 8.0 m × 8.0 m × 0.14 m                |
| Mass density:           | 2400 kg/m <sup>3</sup>                |
| Elastic modulus:        | 30 × 10 <sup>9</sup> N/m <sup>2</sup> |
| Poisson ratio:          | 0.2                                   |
| Critical damping ratio: | 0.02                                  |
| Loading:                | 750 N/m <sup>2</sup> over the floor   |

The displacement and acceleration at the centre of the floor are to be calculated considering perfect and imperfect coordination between individuals in the group, converting the floor into a generalised SDOF system

The floor response is dominated by its fundamental mode,  $\sin(\pi x/L_x) \sin(\pi y/L_y)$ . The properties of the generalised SDOF system of the floor can be determined as follows:

|                                |                               |
|--------------------------------|-------------------------------|
| Modal stiffness:               | $M^* = 5376$ kg               |
| Modal stiffness:               | $K^* = 1.098 \times 10^7$ N/m |
| Fundamental natural frequency: | $f_s = 7.16$ Hz               |
| The generalised load:          | $F = 19,454$ N                |

The displacements and accelerations of the generalised SDOF system are calculated using Equations (9) and (10). The load frequency is set at one-third of the floor frequency, which creates a resonant situation at the third Fourier term. Other parameters are selected as in Table 7.

**Table 7.** Other parameters.

| $\sigma_\psi$ | $a$ | $\sigma_\lambda$ |
|---------------|-----|------------------|
| 0.28π         | 0.6 | 0.05             |

According to  $\sigma_\psi = 0.28\pi$ , crowd reduction factors  $C_\psi(n)$  for different Fourier terms can be found in Table 1 and are presented in Table 8.

**Table 8.** Crowd reduction factors  $C_\psi(n)$ .

| $n$   |       |       |       |
|-------|-------|-------|-------|
| 1     | 2     | 3     | 4     |
| 0.680 | 0.212 | 0.031 | 0.002 |

Based on  $a = 0.6$  and the conclusions about  $\sigma_\delta$ , the synchronization reduction factors  $C_\delta(n)$  for different Fourier terms can be found in Table 3 and are presented in Table 9.

**Table 9.** Crowd reduction factors  $C_\delta(n)$ .

| $n$   |       |       |       |
|-------|-------|-------|-------|
| 1     | 2     | 3     | 4     |
| 1.400 | 0.367 | 0.111 | 0.060 |

According to  $\sigma_\lambda = 0.05$ ,  $\xi = 0.02$ , and the resonant situation at the third Fourier term, the frequency reduction factor  $C_\lambda(n, \xi)$  for different Fourier terms can be found from Tables 5 and 6 and are presented in Table 10.

**Table 10.** Crowd reduction factors  $C_\lambda(n, \xi)$ .

| $n$                            |                                |                              |                                |
|--------------------------------|--------------------------------|------------------------------|--------------------------------|
| 1<br>( $1 \cdot f_p/f_s=1/3$ ) | 2<br>( $2 \cdot f_p/f_s=2/3$ ) | 3<br>( $3 \cdot f_p/f_s=1$ ) | 4<br>( $4 \cdot f_p/f_s=4/3$ ) |
| 1.125                          | 1.806                          | 13.860                       | 1.339                          |

Substituting the structure date, loading date, and reduction factors into Equations (17) and (22), the mean of the random displacement  $A_R(t)$  of the structure is

$$E[A_R(t)] = 1.772 \times 10^{-3} \left[ 1.0 + 1.071 \sin(2\pi f_p t - 0.015) + 0.141 \sin(4\pi f_p t - 1.619) + 0.048 \sin(6\pi f_p t - 4.712) + 0.00015 \sin(8\pi f_p t - 1.5023) \right] \quad (24)$$

The acceleration is

$$E[\ddot{A}_R(t)] = -1.772 \times 10^{-3} \left[ 241 \sin(2\pi f_p t - 0.015) + 127 \sin(4\pi f_p t - 1.619) + 97 \sin(6\pi f_p t - 4.712) + 0.538 \sin(8\pi f_p t - 1.5023) \right] \quad (25)$$

Substituting the structure date and loading data into Equations (9) and (10), the deterministic displacement and acceleration response of the structure can also be obtained. Comparing the results presented in Equations (24) and (25), Figures 4 and 5 present the displacement and acceleration results. The maximum deterministic displacement is 0.0067 m and the max mean of the random displacement is 0.0044 m. The maximum deterministic acceleration is 3.018 m/s<sup>2</sup> and the max mean of the random acceleration is 0.998 m/s<sup>2</sup>.

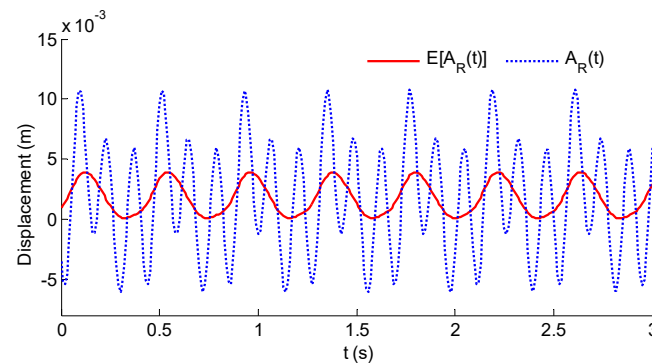


**Figure 4.** Displacement of the structure.

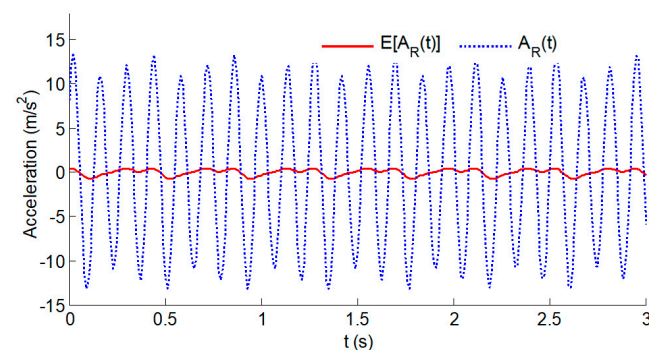


**Figure 5.** Acceleration of the structure.

If the values of  $\sigma_\psi$ ,  $\sigma_\delta$ , and  $\sigma_\psi$  are negligible, such as  $\sigma_\psi = 0.02$ ,  $\sigma_\delta = 0.002$ , and  $\sigma_\psi = 0.002$ , Figure 6 shows the displacement response of the structure. When the deviation of the random variables  $\Delta a$ ,  $\Delta t_s$ , and  $\Delta f_p$  are small, the deterministic displacement is equal to the mean of the random displacement as presented in Figure 6, which meets the expectation. To some degree, this also verifies the correction of Equations (17) and (22), and the coefficients in Tables 1–6.

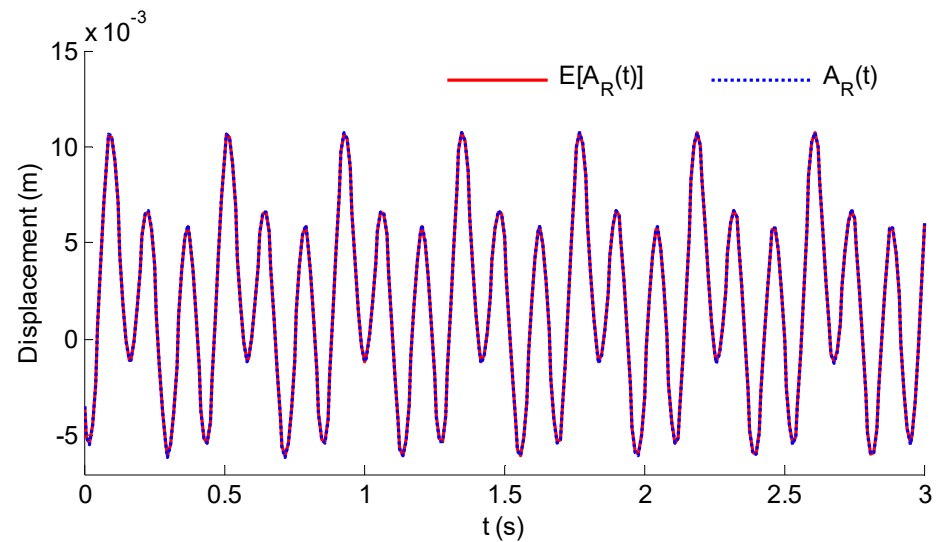


**Figure 6.** Displacement of the structure with  $\sigma_\psi = 0.02$ ,  $\sigma_\delta = 0.002$ , and  $\sigma_\psi = 0.002$ .

In order to appreciate the effect of the two reduction factors, the values of the following term is evaluated,

$$s_n = C_\delta(n)C_\psi(n)C_\lambda(n, \xi) \quad (26)$$

$$\ddot{s}_n = (2n\pi f_p)^2 C_\delta(n)C_\psi(n)C_\lambda(n, \xi) \quad (27)$$

The coefficient  $s_n$  is the harmonic term coefficients to the mean of the random displacement  $A_R(t)$ , and  $\ddot{s}_n$  to the mean of the random acceleration  $\ddot{A}_R(t)$ . The contribution of each of the harmonic terms to the displacement and acceleration, respectively, are shown in Tables 11 and 12.

**Table 11.** Displacement response contributions from each of the harmonic terms.

| Situation  | The Harmonic Terms $n$ |       |       |         |
|--|------------------------|-------|-------|---------|
|  | 1                      | 2     | 3     | 4       |
| Without considering $\Delta a, \Delta t_s, \Delta f_p$ | 1.580                  | 0.611 | 3.382 | 0.036   |
| Considering $\Delta a$                                 | 1.575                  | 0.659 | 2.759 | 0.077   |
| Considering $\Delta t_s$                               | 1.074                  | 0.130 | 0.104 | 0.000   |
| Considering $\Delta f_p$                               | 1.580                  | 0.616 | 1.871 | 0.038   |
| Considering $\Delta a, \Delta t_s, \Delta f_p$         | 1.071                  | 0.141 | 0.048 | 0.00015 |

It can be observed from the results in Table 11 that:

- For perfect coordination when  $\Delta a$ ,  $\Delta t_s$ , and  $\Delta f_p$  are not considered, the response induced by the third load term dominates the total response.
- When contact ratio difference  $\Delta a$  is considered, the resonant response due to the third term becomes smaller. However, the response induced by the third load term also dominates the total response.

- When time delay  $\Delta t_s$  is considered, the resonant response due to the third term becomes much smaller and is even smaller than that induced by the first load component. Therefore, the total response contains more from the response due to the load term.
- When frequency difference  $\Delta f_p$  is considered, the response due to the third term becomes smaller and is a little bit bigger than that induced by the first load component. Hence, the total response contains more from the response due to the load term.
- When  $\Delta a$ ,  $\Delta t_s$ , and  $\Delta f_p$  are taken into account, the response induced by the third load term is further reduced. Thus, the response from the first component is clearer in the total response.

It can be observed from the results in Table 12 that:

- For perfect coordination, the response induced by the third load term dominates the total response. Figure 5 shows the maximum acceleration is up to 1.5 g, which is unrealistic.
- When contact ratio difference  $\Delta a$  is considered, the resonant acceleration due to the third term becomes smaller. However, the acceleration induced by the third load term also dominates the total response.
- When time delay  $\Delta t_s$  is considered, it significantly attenuates the acceleration. The total response contains more from the response due to the load term.
- When frequency difference  $\Delta f_p$  is considered, the acceleration induced by the third load term dominates the total response.
- When  $\Delta a$ ,  $\Delta t_s$ , and  $\Delta f_p$  are considered, the maximum acceleration is further reduced to 0.1 g. Again, the response is controlled by the first term.

**Table 12.** Acceleration response contributions from each of the harmonic terms.

| Situation  | <i>n</i> |     |      |       |
|--|----------|-----|------|-------|
|  | 1        | 2   | 3    | 4     |
| Without considering $\Delta a, \Delta t_s, \Delta f_p$ | 355      | 550 | 6842 | 129   |
| Considering $\Delta a$                                 | 354      | 592 | 5581 | 275   |
| Considering $\Delta t_s$                               | 241      | 117 | 211  | 0.239 |
| Considering $\Delta f_p$                               | 355      | 554 | 3786 | 136   |
| Considering $\Delta a, \Delta t_s, \Delta f_p$         | 241      | 127 | 97   | 0.538 |

## 7. Conclusions

This article studies the design method for evaluating the random response of structures under the load of rhythmic crowds. The load model considers three random variables that reflect incomplete synchronization: time delay, contact ratio, and load frequency. The stochasticity of the structural response is considered by introducing the crowding reduction coefficient, the synchronization reduction coefficient, and the resonance reduction coefficient. The conclusions drawn from this study are that:

- The smaller the standard deviation, the larger the group reduction coefficient, and the smaller the dynamic group effect, which corresponds to better coordination among individuals in the group. The higher the order of the load term, the smaller the crowd reduction coefficient, and the larger the dynamic crowd effect.
- The larger the average overlap, the smaller the synchronization reduction coefficient, and the larger the dynamic crowd effect. The effect of overlap difference on synchronization is not significant. The larger the order of the Fourier term, the smaller the synchronization reduction factor, and the larger the dynamic crowd effect.
- For the resonance reduction coefficient, the larger the standard deviation, the smaller the resonance reduction coefficient, and the larger the dynamic crowd effect. The larger the critical damping ratio, the larger the resonant reduction coefficient, and the smaller the dynamic crowd effect.

- The effect of the standard deviation of the frequency changes and the damping ratio on non-resonant reduction coefficients can be ignored.

**Author Contributions:** Methodology, M.Y.; Software, J.-K.D.; Validation, J.-K.D.; Investigation, M.Y.; Data curation, J.-K.D.; Writing – original draft, J.-K.D.; Supervision, J.-K.D. and M.Y. All authors have read and agreed to the published version of the manuscript.

**Funding:** This research was funded by Guangzhou Basic Research Program, grant number SL2022A03J00954, and the APC was funded by Guangzhou Basic Research Program grant number SL2022A03J00954.

**Data Availability Statement:** No new data were created or analyzed in this study. Data sharing is not applicable to this article.

**Acknowledgments:** I would like to express my deepest gratitude to all those who have supported me throughout this research journey.

**Conflicts of Interest:** The author of this paper with title of Design for Random Response of Structures Subject to Rhythmic Crowd Loading receives research funding by Guangzhou Basic Research Program (SL2022A03J00954). Any opinions, findings, and conclusions expressed in this paper are those solely of the authors and do not necessarily reflect the view of Guangzhou University. The authorship arrangement has been reviewed and approved by Guangzhou University in accordance with its policy on objectivity in research.

## References

1. 'Structural Safety 2000-01'; The 13th Report of the Standing Committee on Structural Safety (SCOSS); Institution of Structural Engineers: London, UK, 2001.
2. Bruno, L.; Corbetta, A. Uncertainties in crowd dynamic loading of footbridges: A novel multi-scale model of pedestrian traffic. *Eng. Struct.* **2017**, *147*, 545–566. [[CrossRef](#)]
3. Allen, D.E.; Rainer, J.H.; Pernica, G. Vibration criteria for assembly occupancies. *Can. J. Civ. Eng.* **1985**, *12*, 617–623. [[CrossRef](#)]
4. Ellis, B.R.; Ji, T. Loads generated by jumping crowds: Numerical modelling. *Struct. Eng.* **2004**, *82*, 35–40.
5. Georgiou, L.; Racic, V.; Brownjohn, J.M.; Elliot, M.T. Coordination of Groups Jumping to Popular Music Beats. *Conf. Proc. Soc. Exp. Mech. Ser.* **2015**, *2*, 283–288.
6. Racic, V.; Brownjohn, J.M.W.; Pavic, A. Measurement and Application of Bouncing and Jumping Loads Using Motion, Tracking Technology. *Conf. Proc. Soc. Exp. Mech. Ser.* **2011**, *63*, 201–210.
7. Yao, S.P.; Wright, J.; Pavic, A.; Reynolds, P. Forces generated when bouncing or jumping on a flexible structure. In Proceedings of the International Conference on Noise and Vibration Engineering, Leuven, Belgium, 16–18 September 2002; VOLS, 1–5; Katholieke Universiteit Leuven: Leuven, Belgium, 2002.
8. Sim, J.; Blakeborough, A.; Williams, M.S. Dynamic loads due to rhythmic human jumping and bobbing. In Proceedings of the 6th International Conference on Structural Dynamics, Paris, France, 4–7 September 2005; VOLS 1–3; Millpress Science Publishers: Rotterdam, The Netherlands, 2005; Volume 1, pp. 467–472.
9. Duarte, E.; Ji, T. Action of Individual Bouncing on Structures. *J. Struct. Eng.* **2009**, *135*, 818–827. [[CrossRef](#)]
10. Ellis, B.R.; Ji, T. *The Response of Structures to Dynamic Crowd Loads*; The Building Research Establishment Ltd.: Watford, UK, 2004.
11. Sim, J.; Blakeborough, A.; Williams, M.; Parkhouse, G. Statistical Model of Crowd Jumping Loads. *J. Struct. Eng.* **2008**, *134*, 1852–1861. [[CrossRef](#)]
12. Vijayan, A.; Abraham, N.M.; Da Anitha Kumari, S. Analysis of structures subjected to crowd loads. *Procedia Struct. Integr.* **2019**, *14*, 696–704. [[CrossRef](#)]
13. Bruno, L.; Venuti, F. A Simplified Serviceability Assessment of Footbridge Dynamic Behaviour Under Lateral Crowd Loading. *Struct. Eng. Int.* **2010**, *20*, 442–446. [[CrossRef](#)]
14. Ji, T.; Ellis, B.R. Floor vibration induced by dance type loads: Theory. *Struct. Eng.* **1994**, *72*, 37–44.
15. Ellis, B.R.; Ji, T. Floor vibrations induced by dance type loads—Verification. *Struct. Eng.* **1994**, *72*, 45–50.
16. Willford, M. An investigation into crowd-induced vertical dynamic loads using available measurements. *Struct. Eng.* **2001**, *79*, 21–25.
17. Gaspar, C.; da Silva, J.G.S. Influence of the Human Rhythmic Activities Modelling on the Composite Floors Dynamic Response. *J. Civil Eng. Architect. Res.* **2015**, *2*, 429–437.
18. BS6399; Loading for Buildings. Part 1: Code of Practice for Dead and Imposed Loads. British Standards Institution (BSI): London, UK, 1996.
19. Institution of Structural Engineers (Istructe). *Dynamic Performance Requirements for Permanent Grandstands Subjected to Crowd Action: Interim Guidance for Assessment and Design*; Institution of Structural Engineers: London, UK, 2001.
20. Ellis, B.R. *Loads Generated by Jumping Crowds: Numerical Assessment*; The Structural Engineer: Hong Kong, China, 2003.

21. Ellis, B.R.; Ji, T. *Loads Generated by Jumping Crowds: Experimental Assessment*; BRE IP 4/02; The Structural Engineer: Hong Kong, China, 2002; 12p.
22. Tan, H.; Zhao, Y.; Chen, J. Experiment investigation of coherency factor of rhythmic jumping and its application for simulation of crowd jumping load. In Proceedings of the 5th International Conference on Computational Methods in Structural Dynamics and Earthquake Engineering, Crete Island, Greece, 25–27 May 2015.
23. Chen, J.; Wang, L.; Chen, B.; Yan, S. Dynamic properties of human jumping load and its modelling: Experimental study. *J. Vib. Eng.* **2014**, *27*, 16–24. (In Chinese)

**Disclaimer/Publisher's Note:** The statements, opinions and data contained in all publications are solely those of the individual author(s) and contributor(s) and not of MDPI and/or the editor(s). MDPI and/or the editor(s) disclaim responsibility for any injury to people or property resulting from any ideas, methods, instructions or products referred to in the content.